

# Consistently modeling the combined effects of temperature and concentration on nitrate uptake in the ocean

S. Lan Smith<sup>1</sup>

---

<sup>1</sup> Environmental Biogeochemical Cycles Research Program, RIGC, JAMSTEC, 3173-25 Showa-machi, Kanazawa-ku, Yokohama-shi Kanagawa-ken, Japan 236-0001 (lanimal@jamstec.go.jp)

**Abstract.** Considerable uncertainty remains about the combined effects of multiple limiting factors on oceanic phytoplankton, which constitute the base of the marine food web and mediate biogeochemical cycles of carbon and nutrients. I apply Bayesian statistical analysis to disentangle the combined effects of temperature and concentration on uptake of the important nutrient nitrate as measured by oceanic field experiments. This provides consistent estimates of temperature sensitivities for the maximum uptake rate and affinity (initial slope), the two parameters which define the shape of the uptake-concentration curve. No evidence is found that the temperature sensitivities of these two parameters differ, which implies that half-saturation constants, as commonly obtained by fits of the Michaelis-Menten (MM) equation, should be independent of temperature. This explains the robust relationship between half-saturation values and ambient nitrate concentration observed in compilations of data from diverse studies of uptake in marine and freshwater environments. Compared to the MM kinetics as applied in most large-scale models, accounting for a physiological trade-off between maximum uptake rate and affinity: (1) yields a more consistent model, which better describes observed changes in the shape of the uptake-concentration curve, and (2) implies a significantly greater inferred temperature sensitivity for nitrate uptake. These findings impact our understanding of how marine ecosystems and biogeochemical cycles will respond to climate change and anthropogenic nutrient inputs, both of which are expected to alter the relationship between nutrient concentrations and temperature in the near-surface ocean.

## 1. Introduction

1 Accurate representations of the temperature dependence of biological processes are es-  
2 sential if we are to understand the direct effects and associated feedbacks of natural  
3 physical variability, anthropogenic nutrient inputs and climate change on ecosystems and  
4 biogeochemical cycles. Most of our current knowledge about the temperature dependence  
5 of phytoplankton processes comes from laboratory experiments with single-species cul-  
6 tures. Few data sets from field studies even exist which allow directly testing whether  
7 those results can be extrapolated to the real ocean. However, accounting for the com-  
8 bined effects of multiple limiting factors implies different patterns for growth [Moisan  
9 et al., 2002] and nutrient uptake [Smith, 2010] by phytoplankton in the ocean.

10 Eppley [1972] estimated the temperature dependence of maximum potential growth rate  
11 for phytoplankton by fitting to the “top of the data” (fastest growth rate measured at each  
12 temperature) using a compilation of data from many single-species culture experiments,  
13 reasoning that this would exclude the effects of other potential limiting factors such as  
14 nutrients and light. Statistical analysis of a more extensive data set has recently confirmed  
15 this exponential dependence, with slight modification of its parameters [Bissinger et al.,  
16 2008]. However, Eppley [1972] noted that this overall exponential dependence contrasts  
17 with the steep decrease in growth rate typically observed for any single species above its  
18 species-specific optimal temperature,  $T_o$ . Recently some complex large-scale models do  
19 resolve distinct values of  $T_o$  for different species [e.g., Follows et al., 2007] or functional  
20 types [e.g., LeQuere et al., 2005]. However, such models are too computationally demand-  
21 ing for direct use in long-term studies of biogeochemical cycles and climate, although they

22 may provide valuable information and parameterizations that can be useful for long-term  
23 studies with other models. Therefore, many large-scale models assume exponential tem-  
24 perature dependence, multiplied by other limiting factors, for nutrient uptake, growth  
25 and other biological processes [e.g., Fasham et al., 1993; Aumont et al., 2003; Kishi  
26 et al., 2007]. The best justification for this assumption is that it represents the ecological  
27 dependence, under the assumption that at ambient environmental temperature,  $T_a$ , the  
28 dominant species will have optimal temperature  $T_o = T_a$  [Eppley, 1972]. On the other  
29 hand, many oceanic biogeochemical models [e.g., Yamanaka and Tajika, 1996; Parekh  
30 et al., 2005; Marinov et al., 2008] assume no temperature dependence for nutrient uptake.

31 Here I test assumptions about the combined effects of temperature and nutrient con-  
32 centration on uptake rate against an extensive data set for nitrate uptake as measured  
33 in field experiments [Harrison et al., 1996]. This addresses the overall (ecological) tem-  
34 perature dependence across the various species that dominate at different locations and  
35 seasons, not the dependence for any given species. I test the hypothesis that the param-  
36 eters of uptake kinetics (i.e., the shape of the uptake-concentration curve), as determined  
37 in typical short-term incubation experiments, depend on both temperature and ambient  
38 nutrient concentration. I consider two representations of the dependence of these up-  
39 take parameters on concentration: (1) the assumption of fixed physiology inherent in the  
40 widely-applied Michaelis-Menten (MM) kinetics, which assumes no dependence of these  
41 parameters on ambient nutrient concentration, and (2) the recently developed Optimal  
42 Uptake (OU) kinetics, based on a physiological trade-off between maximum uptake rate  
43 and affinity for nutrient (assuming that physiology and hence the shape of the uptake-  
44 concentration curve depend on the ambient nutrient concentration). I apply the Adaptive

45 Metropolis algorithm [Haario et al., 2001; Laine, 2008], an automatic Bayesian statisti-  
46 cal method, to assess how well each set of assumptions agrees with the data set as a  
47 whole. This reveals that OU kinetics: (1) better describes the patterns of variation for  
48 the uptake parameters, which depend on both temperature and nutrient concentration,  
49 and (2) implies a greater sensitivity of these parameters to temperature than does MM  
50 kinetics. It further reveals no evidence that the temperature sensitivities of maximum  
51 uptake rate and affinity differ, which explains the lack of any consistent dependence of  
52 MM half-saturation constants on temperature (at least at the large scale).

## 2. Methods

### 2.1. Theory

53 For phytoplankton and other microorganisms, the Michaelis-Menten (MM) equation is  
54 most commonly applied to describe the dependence of uptake rate on nutrient concentra-  
55 tion [Dugdale, 1967; Harrison et al., 1996]:

$$V_{MM} = \frac{V_{\max}S}{K_s + S} \quad (1)$$

56 where  $V_{MM}$  is the uptake rate,  $S$  is the nutrient concentration, and  $K_s$  is the MM half-  
57 saturation constant for nutrient  $S$ . This equation is often combined with Arrhenius-  
58 type [Goldman and Carpenter, 1974] or similar exponential [Eppley, 1972] temperature  
59 dependence for  $V_{\max}$ .

60 Compared to Eq. (1), Affinity-based kinetics provides a more natural and theoretically  
61 well-founded representation of uptake [Aksnes and Egge, 1991]. Affinity,  $A$ , is defined as  
62 the initial slope of rate versus concentration at low nutrient concentrations [Healey, 1980],

63 so that:

$$V_A = \frac{V_{\max}AS}{V_{\max} + AS} \quad (2)$$

64 Aksnes and Egge [1991] showed that MM kinetics is equivalent to affinity-based kinetics  
 65 under the assumption of fixed physiology (no acclimation in response to changing nutrient  
 66 concentrations); i.e., for constant  $V_{\max}$  and  $A$ , Eq. (2) is mathematically equivalent to Eq.  
 67 (1). Furthermore, Eq. (2) with temperature dependent  $V_{\max}$  and  $A$  is equivalent to Eq.  
 68 (1) with temperature dependent  $V_{\max}$  and  $K_s$ . If  $V_{\max}$  and  $A$  share identical temperature  
 69 dependence,  $K_s$  must be independent of temperature.

70 However, experiments with various single-species cultures have found temperature de-  
 71 pendent  $K_s$  for uptake of nitrogen, phosphorus and silicon [Eppley et al., 1969; Dauta,  
 72 1982]. Therefore, I examine the possibility of distinct temperature sensitivities for  $V_{\max}$   
 73 and  $A$ , by defining energies of activation,  $E_{a,V}$  and  $E_{a,A}$ , respectively, such that:

$$V_{\max} = V_{\max,r} \exp\{-(1/T - 1/T_r)E_{a,V}/R\} \quad (3a)$$

$$A = A_r \exp\{-(1/T - 1/T_r)E_{a,A}/R\} \quad (3b)$$

75 where  $T$  is temperature in K,  $R$  is the gas constant, and  $V_{\max,r}$  and  $A_r$  are the values of  
 76  $V_{\max}$  and  $A$ , respectively, at reference temperature  $T_r$ . If  $E_{a,A} = E_{a,V}$ , one set of Arrhe-  
 77 nius terms cancels out after substitution into Eq. (2), leaving only one Arrhenius term  
 78 in the numerator, which is equivalent to the widely applied assumption of temperature  
 79 dependence only for  $V_{\max}$  [Goldman and Carpenter, 1974].

80 Optimal Uptake (OU) kinetics extends Eq. (2) to include a physiological trade-off,  
 81 whereby phytoplankton allocate internal resources to increase either  $V_{\max}$  or  $A$ , at the  
 82 expense of reducing the other [Pahlow, 2005; Smith et al., 2009].  $V_0$  and  $A_0$  are defined  
 83 as the potential maximum values of  $V_{\max}$  and  $A$ , respectively, and their actual values are

84 determined by physiological acclimation to the ambient concentration of growth-limiting  
 85 nutrient. The data examined here [W. G. Harrison et al., 1996] were from typical short-  
 86 term uptake experiments [P. J. Harrison et al., 1989], in which a series of incubations  
 87 with graded nutrient additions is conducted for each sample taken from water having  
 88 ambient nutrient concentration,  $S_a$ . Assuming that phytoplankton were pre-acclimated  
 89 to  $S_a$ , OU kinetics gives the following equations for the dependence on  $S_a$  of affinity-based  
 90 parameters, as measured by short-term experiments during which the phytoplankton do  
 91 not have time to acclimate [Smith et al., 2009; Smith, 2010]:

$$V_{\max} = \frac{\sqrt{\frac{A_0 S_a}{V_0}}}{1 + \sqrt{\frac{A_0 S_a}{V_0}}} V_0 \quad (4)$$

$$A = \frac{1}{1 + \sqrt{\frac{A_0 S_a}{V_0}}} A_0 \quad (5)$$

93 Note that  $S_a$ , the ambient concentration in the ocean, is not the concentration  $S$  in the  
 94 short-term incubation experiments using graded nutrient additions. This predicts that  
 95 such short-term experiments will measure values of  $V_{\max}$  that increase with  $S_a$  and values  
 96 of  $A$  that decrease with increasing  $S_a$ . For temperature dependence with OU kinetics I  
 97 apply Arrhenius terms for  $V_0$  and  $A_0$ , respectively, by defining  $E_{a,V}$ ,  $E_{a,A}$ ,  $V_{0,r}$  and  $A_{0,r}$ ,  
 98 exactly analogous to the above treatment for  $V_{\max}$  and  $A$  with MM kinetics Eqs. (3a and  
 99 3b).

## 2.2. Data

100 Data were those of Harrison et al. [1996] as rearranged by Smith [2010] to match ob-  
 101 served ambient temperatures and nitrate concentrations to the reported values of  $V_{\max}$   
 102 ( $n = 60$ ) and  $K_s$  ( $n = 48$ ) as obtained from their short-term ( $\sim 3$ h) incubation experi-  
 103 ments. At each of the locations, which covered the North Atlantic ocean, graded nutrient

104 additions were made to separate bottles containing sampled seawater, which were then  
105 incubated ship-board at ambient temperature in order to measure nutrient uptake rates.  
106 They calculated parameters of the MM equation for nutrient uptake by fitting to the data  
107 so obtained locally, i.e., for the set of experiments conducted at each location, respectively.  
108 I calculate values of affinity as  $A = V_{\max}/K_s$ . For the set of short-term experiments con-  
109 ducted using each ambient water sample, respectively, the MM equation described the  
110 shape of the uptake response well, albeit with different values of  $V_{\max}$  and  $K_s$  for different  
111 water samples [Harrison et al., 1996]. Either Eq. (1) or Eq. (2) describes this same shape,  
112 the only difference being whether  $K_s$  or  $A$  is employed.

## 2.3. Fitting

### 113 2.3.1. General Approach

114 The Adaptive Metropolis (AM) algorithm [Haario et al., 2001; Laine, 2008] yields a  
115 consistent Bayesian statistical interpretation of the data set as a whole, providing a way to  
116 disentangle the combined effects of temperature and nutrient concentration. I chose to fit  
117 the affinity-based Eq. (2) to the data, because this equation allows a concise representation  
118 of both MM and OU kinetics, whereas expressing OU kinetics in terms of  $K_s$  using Eq.  
119 (1), although possible, is cumbersome and counter-intuitive.

120 Two cases are examined: (1) the 'Affinity model' assuming no physiological acclimation  
121 (equivalent to MM kinetics) and (2) the 'OU model' assuming physiological acclimation  
122 according to OU kinetics. Arrhenius-type temperature dependence was assumed for max-  
123 imum uptake rate and affinity, respectively.

124 For the Affinity model, the temperature dependent expressions for  $V_{\max}$  and  $A$  were  
125 fitted to the respective data values, using the corresponding values of ambient temper-

126 ature and ambient nitrate concentration as independent variables. For OU kinetics, the  
127 temperature dependent expressions for  $V_0$  and  $A_0$  were substituted into the short-term  
128 approximations for their dependence on ambient nutrient concentration, Eqs. (4) and (5),  
129 respectively. The resulting equations were fitted to the data in the same way as for the  
130 Affinity model.

### 131 **2.3.2. Adaptive Metropolis algorithm**

132 The Adaptive Metropolis (AM) algorithm [Haario et al., 2001; Laine, 2008], includ-  
133 ing Gibbs sampling to estimate the distribution of the standard error (variance) of each  
134 observation type [Laine, 2008], was used to fit each set of equations to the data. This  
135 algorithm is for the most part automatic and non-parametric; i.e., there are few arbitrary  
136 constants to be adjusted by the user. This provides a consistent comparison of each model,  
137 respectively, with the data set as a whole.

138 In this application, Gibbs sampling provides weights for each data type, based on the  
139 mismatch between model and data, so that the ensemble of the fitted model output  
140 (posterior distribution) matches the distribution of the data. Specifically, if the model-  
141 data mismatch (residuals) for each data type  $o$  is a Normally (Gaussian) distributed  
142 random variable with mean zero and variance  $\sigma_o$  and the prior estimate of  $1/\sigma_o^2$  is assumed  
143 to have a Gamma distribution, then the conditional distribution for each  $1/\sigma_o^2$  (given  
144 the data and model) is also a Gamma distributed random variable [Carlin and Louis,  
145 1996; Gelman et al., 2004]. Here Gibbs sampling exploits this property, called conjugacy  
146 of the prior and conditional distributions, to sample the posterior distribution of  $1/\sigma_o^2$   
147 based on its prior estimate together with information about the distribution of model-

148 data mismatch, which comes from the unweighted sum of squared residuals (Carlin and  
 149 Louis, 1996, Ch. 5; Gelman et al., 2004, Ch. 14).

150 Output includes the sampled distribution of values for each parameter value fitted and  
 151 distributions of the standard errors for each data type. Combining these gives the pre-  
 152 dicted range within which observations should lie, assuming the model is correct [Gelman  
 153 et al., 2004; Laine, 2008].

### 154 2.3.3. Likelihood function

155 The likelihood is calculated as in Laine [2008], based on the probability density function  
 156 of the Gaussian distribution. It includes a prior component (for deviations of parameter  
 157 values from their prior expected values) and a term based on the sum of squared difference  
 158 between the model and data. The log likelihood is thus:

$$\log_e L = \frac{-\log_e((2\pi)^{n_p}|C_p|)}{2} - \frac{\delta_p^T C_p^{-1} \delta_p}{2} + \sum_o \left( -N_o \log_e(\sigma_o \sqrt{2\pi}) - \frac{SS_o(\theta)}{2\sigma_o^2} \right) \quad (6)$$

159 where  $C_p$  is the prior covariance matrix (uncertainty in the prior estimates),  $n_p$  is the  
 160 number of parameters fitted,  $\delta_p = \theta - \eta$  is the vector of deviations of parameter values  
 161  $\theta$  from their prior values  $\eta$ ,  $N_o$  is the number of data points for each observation type  $o$ ,  
 162 and  $SS_o$  is the unweighted sum of squared errors for data type  $o$ . Previous studies found  
 163 that for fits to these data a log transformation is required to make the distribution of  
 164 residuals approximately Gaussian (Normal) [Smith et al., 2009; Smith, 2010]. Therefore,  
 165  $SS_o$  is calculated as:

$$SS_o = \sum_{i=1}^{N_o} (\log_{10} y_i - \log_{10} f(x_i, \theta))^2 \quad (7)$$

166 where  $y_i$  is the  $i$ th observed value (here, of either  $V_{\max}$  or  $A$ ) and  $f(x_i, \theta)$  is the modeled  
 167 value as a function of the corresponding independent variables  $x_i$  (in this case, ambient  
 168 temperature and nitrate concentration) and the parameter values  $\theta$ .

#### 169 **2.3.4. Tests of the algorithm and robustness of results**

170 Identical twin tests confirmed that the algorithm functions correctly and is able to  
 171 constrain the fitted parameters based on this data set. Fits to reduced data sets confirmed  
 172 that the complete data set is more than sufficient to draw the conclusions herein. Methods  
 173 and results are described in the Auxiliary Material.

#### 174 **2.3.5. Model selection**

175 As in other Bayesian methods, the likelihood provides a relative measure of goodness  
 176 of fit, and the Akaike Information Criterion (AIC) [Akaike, 1974] further accounts for the  
 177 trade-off between bias and variance (roughly interpretable as accuracy versus complexity)  
 178 when comparing models having different numbers of parameters. Thus application of  
 179 AIC to compare models in a Bayesian context is analogous to the application of ANOVA  
 180 in a frequentist context to compare linear regression models having different numbers of  
 181 parameters. Here I calculate AICc, which is the AIC corrected for the effects of sample  
 182 size [Burnham and Anderson, 1998; Anderson et al., 2000], using the ensemble mean log  
 183 likelihood ( $\log\bar{L}$ ) for each fitted model, respectively:

$$AICc = -2\log\bar{L} + 2p + \frac{2p(p+1)}{N-p-1} \quad (8)$$

184 where  $p$  is the number of parameters fitted for each model, respectively, and  $N$  is the total  
 185 number of observations.

186 AIC provides only a relative comparison of models; i.e., its absolute value for any  
 187 particular model is not meaningful, but only differences between models. The model with  
 188 the lowest AIC is best, and differences in AIC for each mode,  $m$ , are calculated as:

$$\Delta_{AIC,m} = AIC_m - \min_{i \leq M}(AIC_i) \quad (9)$$

189 where 'min' denotes the minimum value over the total number of models considered ( $M$ ).  
 190 Although  $\Delta_{AIC,m}$  alone can be taken as an approximate measure of the relative support  
 191 for model  $m$  compared to the best model, a quantitative measure in terms of relative  
 192 probability (of each model, respectively, given the observations) is provided by the Akaike  
 193 weights [Burnham and Anderson, 1998; Anderson et al., 2000]:

$$w_m = \frac{\exp\left(\frac{-\Delta_{AIC,m}}{2}\right)}{\sum_i^M \exp\left(\frac{-\Delta_{AIC,i}}{2}\right)} \quad (10)$$

194 Here I adopt the criteria  $w_m > 0.95$  for accepting model  $m$ , and conversely  $w_m < 0.05$   
 195 for rejection. This is not a hypothesis test as widely applied in frequentist statistics,  
 196 but instead a relative ranking of the probabilities of all models considered given the  
 197 observations [Anderson et al., 2000]. As an alternative, the Bayesian Information Criterion  
 198 (BIC) could instead be used to calculate these weights, which would tend to favor more  
 199 parsimonious models more strongly than does the AIC [Schwarz, 1978; Congdon, 2001].

### 200 2.3.6. Parameters for the algorithm

201 The prior covariance matrix,  $C_p$ , for parameters was chosen not to be very restrictive,  
 202 by assuming a coefficient of variation of 2.0 for each parameter estimate, respectively.  
 203 Thus, the diagonal element (variance) corresponding to each parameter was assumed to  
 204 be the square of double the prior estimate of that parameter. Non-diagonal terms were  
 205 taken to be zero (no cross-correlations). Prior estimates for temperature sensitivity,  $E_a/R$ ,  
 206 were taken as  $5.7 \times 10^3$  K, which for a  $10^\circ\text{C}$  increase in temperature from 283 K to 293  
 207 K corresponds to a doubling of rate. Prior estimates for  $V_{\max}$  and  $A$  at the reference  
 208 temperature,  $T_r = 293$  K, were taken as the maximum observed values of each parameter,  
 209 respectively.

210 For the Gibbs sampling [Laine, 2008], parameter  $n_0$ , which represents the prior uncer-  
211 tainty of observations, was taken as unity, and parameter  $S_0$ , the prior mean for each  $\sigma$ ,  
212 was taken as 0.01 based on trial fits. The results of fits were not sensitive to the specific  
213 choice of these parameters for any  $S_0 \lesssim 1$ . (For larger values of  $S_0$  the fits were not  
214 constrained because the resulting large values of  $\sigma$  gave very low weights to the data.)  
215 Because the sum of squares is calculated in log space as per equation (7) above, the  
216 algorithm samples the distribution of standard errors in log space as well.

### 217 **2.3.7. Numerical calculations**

218 Uniform  $(0, 1)$  pseudo-random numbers were generated using the Mersenne twister  
219 algorithm, as originally coded by Takuji Nishimura, in 1997, and later translated to  
220 FORTRAN90 by Richard Woloshyn, in 1999. From these the Gaussian (Normal)  
221 pseudo-random numbers, multivariate Gaussian pseudo-random numbers, and Gamma-  
222 distributed pseudo-random numbers needed for the AM algorithm were generated us-  
223 ing the algorithms of Gentle [2003], which I coded into FORTRAN90. Cholesky de-  
224 compositions and matrix inversions were calculated using, respectively, the CHOLESKY  
225 [Healy, 1968b] and SYMINV [Healy, 1968a] routines, as coded into FORTRAN90 by John  
226 Burkardt, in 2008.

## **3. Results**

### **3.1. Correlation of temperature and nitrate concentration**

227 Ambient values of observed temperature and nitrate concentration are strongly and  
228 significantly negatively correlated in this data set (Fig. 1). Such negative relationships  
229 are a general feature of the near-surface ocean, although they differ quantitatively with  
230 location [Silio-Calzada et al., 2008]. Smith [2010] found a similar negative relationship

231 between temperature and nitrate concentration in the data set of Kanda et al. [1985] from  
232 the North Pacific.

### 3.2. Distinct vs. identical temperature sensitivities

233 Fits of the Affinity-based and OU equations for kinetic parameters, assuming distinct  
234 temperature sensitivities for  $V_{\max}$  and  $A$  (Fig. 2) resulted in lower log likelihoods (Table  
235 1) than fits assuming the same temperature sensitivities (for either model, respectively).  
236 This is because increasing the number of parameters reduces the likelihood slightly through  
237 the prior contribution, which accounts for deviations of parameter values from their prior  
238 estimates. Values of Akaike Information Criteria (AIC) [Akaike, 1974] differ even more,  
239 because AIC accounts for the added uncertainty associated with the additional parameter  
240 required to account for distinct temperature sensitivities.

241 The models with distinct temperature sensitivities for  $V_{\max}$  and  $A$  both have probabili-  
242 ties less than 0.01 based on the Akaike weights (Table 2) and are therefore rejected. Thus  
243 there is no evidence that the temperature sensitivities of  $V_{\max}$  and  $A$  differ, and therefore  
244 no evidence that  $K_s$  depends on temperature in this data set. Note that here I address  
245 the overall (ecological) temperature dependence across the various species that dominate  
246 at different locations and seasons, and not the dependence for any given species.

247 The OU model assuming the same temperature sensitivity for  $V_{\max}$  and  $A$  has an Akaike  
248 weight,  $w > 0.95$  (Table 2), and is therefore accepted as the model which best agrees with  
249 the observations. For the models differing only in the assumption of identical versus  
250 distinct temperature sensitivities for  $V_{\max}$  and  $A$ , results differ most for  $A$  in the model  
251 assuming no physiological trade-off (Fig. 2C versus Fig. 3C) and for the resulting values  
252 of  $K_s$  (Fig. 2E versus Fig. 3E). The Affinity model fits the observed data by making

253 the temperature sensitivity of  $A$  much greater than that of  $V_{\max}$ , which results in a steep  
254 decrease in  $K_s$  with increasing temperature (Fig. 2E). Fits to only the data for  $T > 285$   
255 K (not shown) give the same pattern with a similarly strong temperature sensitivity for  
256  $A$ , confirming that this is not a result only of the relatively few values of affinity at low  
257 temperatures.

### 3.3. Physiological trade-off vs. fixed physiology

258 The model assuming the physiological trade-off of OU kinetics agrees significantly better  
259 with the data than the model without this trade-off (Table 2). This is particularly evident  
260 when the fitted kinetic parameters are plotted versus ambient nitrate concentration (Fig.  
261 4). Correlations of the best-fit values of  $V_{\max}$  with their corresponding observed values are  
262 slightly better for the Affinity model than for the OU model, but the OU model's best-fit  
263 values of  $A$  are more strongly correlated with the observations by a greater margin (Table  
264 3). Whether the temperature sensitivities of  $V_{\max}$  and  $A$  were assumed to be the same  
265 or distinct made little difference in these correlations for the OU model. In all cases, the  
266 ensemble mean values (not shown) of model output (kinetic parameters) were practically  
267 indistinguishable from the corresponding best-fit values.

### 3.4. Combined effects of temperature and concentration

268 With the Affinity model values of kinetic parameters do not depend on the ambient  
269 nitrate concentration (Fig. 4), and the inferred temperature sensitivity ( $E_a/R$ ), is lower  
270 than with the OU model (Table 1). The apparent dependence (Figs. 4A and 4C) results  
271 from the correlation of ambient nitrate concentration and temperature; i.e., at high nitrate

272 concentrations, temperature tends to be low, which results in a tendency for lower  $V_{\max}$   
273 and  $A$  at high nitrate concentrations.

274 The differences in inferred temperature sensitivities for the Affinity model versus the OU  
275 model result directly from the combined effects of temperature and concentration on the  
276 values of  $V_{\max}$  and  $A$  in the equations of the OU model, in contrast to the the dependence  
277 of these parameters on only temperature in the Affinity model. In the OU model,  $V_{\max}$   
278 increases with both the ambient temperature and ambient nitrate concentration (Eq. 4),  
279 which means that they tend to have opposing effects, given their negative relationship  
280 in this data set (Fig. 1) and in the near-surface ocean in general [Silio-Calzada et al.,  
281 2008]. This is why the greatest modeled values of  $V_{\max}$  with the OU model occur at  
282 intermediate values of both nitrate concentration (Fig. 4B) and temperature (Figs. 2B  
283 and 3B), in agreement with the observations. This is also why the inferred sensitivity  
284 of  $V_{\max}$  is greater for the OU model; i.e., to obtain approximately the same net effect,  
285 the temperature sensitivity must be greater in order to counteract the dependence on  
286 concentration.

287 It is surprising, however, that the correlation of the best-fit and observed values of  $V_{\max}$   
288 is actually slightly worse for the OU than for the Affinity model (Table 3). There remains  
289 considerable room for improvement, given that neither model explains more than about  
290 20% of the variability in  $V_{\max}$ .

291 On the other hand, in the OU model  $A$  increases with increasing temperature and with  
292 decreasing nitrate concentration (Eq. 5). This is why, under the assumption of distinct  
293 temperature sensitivities for  $V_{\max}$  and  $A$ , the inferred temperature sensitivity is much  
294 greater with the Affinity model than with the OU model; i.e., the higher temperature

295 sensitivity compensates for the lack of dependence of  $A$  on ambient nitrate concentration  
296 in the Affinity model. The correlations of modeled and observed values of  $A$  and  $K_s$ ,  
297 respectively, are greater with the OU model than with the Affinity model, and by a wide  
298 margin under the assumption of identical temperature sensitivities for  $V_{\max}$  and  $A$  (Table  
299 3).

300 The observed and fitted values of kinetic parameters together with observed ambient  
301 nitrate concentration, can be used to estimate the *in situ* uptake rates at ambient con-  
302 ditions. Although neither model represents the full range of estimated *in situ* uptake  
303 rates, the model accounting for the physiological trade-off (Fig. 5B) predicts a slightly  
304 wider range of uptake rates, which agrees better with the estimates based on the reported  
305 kinetic parameters than does the model without physiological acclimation (Fig. 5A).  
306 However, there is no difference in the correlations of the estimates based on the Affinity  
307 and OU models, respectively, with the estimates based on the observed values of kinetic  
308 parameters ( $r^2 = 0.51$  for both models, Fig. 5). This similarity results from the fact  
309 that both models were fitted to the same observations. Although the two models produce  
310 similar estimates of *in situ* uptake rates for the precise values of observed ambient tem-  
311 perature and concentration from this data set, they would produce different results for  
312 different ambient conditions, specifically for a different relationship between temperature  
313 and concentration than that in this data set.

### 3.5. Inhibition of nitrate uptake by ammonium

314 The well known inhibition of nitrate uptake in the presence of ammonium, which was a  
315 major focus of the study by Harrison et al. [1996], deserves mention as a potential determi-  
316 nant of the overall pattern for  $V_{\max}$ . They estimated parameters for this inhibition using

317 incubations with graded additions of isotopically labeled ammonium. As they stated, this  
318 does not directly assess the degree of inhibition *in situ*. Still, it provides the best data  
319 to estimate what that effect might be, specifically for this data set. Using the reported  
320 values of inhibition parameters together with the *in situ* ammonium concentration, the  
321 mean value of inhibition, expressed as the factor ( $0 \leq \gamma \leq 1$ ) by which maximum nitrate  
322 uptake rate would be reduced [Eq. 3 of Harrison et al., 1996], is 0.91 (standard deviation  
323 = 0.10,  $n = 42$ ). This suggests that this inhibition plays a minor role in determining  
324 the overall pattern for  $V_{\max}$  of nitrate uptake. However, these observations are from a  
325 relatively iron-replete region, and ammonium inhibition of nitrate is likely to be stronger  
326 under iron limitation [Armstrong, 1999].

## 4. Discussion

### 4.1. Lack of temperature dependence for $K_s$

327 Whereas Smith et al. [2009] could only present plausible yet somewhat equivocal ar-  
328 guments that the pattern of  $K_s$  was more likely determined by pre-acclimation to the  
329 ambient nutrient concentration rather than by temperature, the results herein make clear  
330 that the explanation in terms of the nutrient concentration is more consistent with the  
331 data set as a whole. This validates the implicit assumption of a constant value for the  
332 ratio  $V_0/A_0$  as applied by Smith [2010] in analyzing the combined effects of temperature  
333 and concentration on  $V_{\max}$  only. Although this validates the widely applied assumption  
334 that  $K_s$  is independent of temperature in models using MM kinetics [Goldman and Car-  
335 penter, 1974], the results herein also clearly show that OU kinetics better reproduces the  
336 observed variations in kinetic parameters compared to the Affinity model. This finding  
337 also explains the robust relationship between  $K_s$  and ambient nitrate concentration as

338 observed in compilations of data from diverse studies of uptake rates in both marine and  
339 freshwater environments [Collos et al., 2005; Smith et al., 2009]. It thus explains why the  
340 prediction of OU kinetics, that  $K_s$  should increase as the square root of ambient nutrient  
341 concentration, agrees with observations from various environments despite differences in  
342 temperature [Smith et al., 2009].

## 4.2. Temperature sensitivity of uptake rate

343 For a simple exponential function such as employed by Eppley [1972], the relative in-  
344 crease for a given change in temperature is constant, whereas for the Arrhenius equation  
345 it depends on the specific temperature interval. The former is sometimes given the short-  
346 hand ' $Q_{10}$ ', e.g., a  $Q_{10}$  of 2 indicates a doubling of rate for a 10 K increase in temperature.  
347 Although the increase varies with temperature in the Arrhenius equation, this makes a  
348 difference of only about 10% over the range of ambient temperatures in the near-surface  
349 ocean. For an increase from 10 to 20°C, the rate increases by 3.1 times for  $E_a/R = 9380$   
350 K (Table 1) versus 2.9 times for 20 to 30°C. For  $E_a$  estimated for the Affinity model, these  
351 values are 1.9 and 1.8 times respectively. Therefore, the best fits of the Arrhenius func-  
352 tion for the two models yield a  $Q_{10}$  of  $\sim 3$  and  $\sim 2$  for the OU and Affinity (MM) models,  
353 respectively. The latter is indistinguishable from the estimate of  $Q_{10}$  for growth [Eppley,  
354 1972; Bissinger et al., 2008] as widely applied for various processes, including uptake, in  
355 ecosystem models. This shows that the temperature sensitivity obtained herein with the  
356 OU model is considerably greater than that commonly applied in ecosystem models.

357 The temperature sensitivity inferred based on OU kinetics is at the high end of the  
358 typical range of  $Q_{10} = 2$  to 3 reported for growth of heterotrophic bacteria [Pomeroy and  
359 Wiebe, 2001]. Further studies are needed to test the combined effects of nutrient con-

360 centration and temperature on phytoplankton growth rates, which may exhibit complex  
 361 interactions, given these results for nutrient uptake and the fact that such interactions  
 362 are well known, although not entirely well understood, for bacteria [Pomeroy and Wiebe,  
 363 2001]. Whether there is in general a difference in the temperature sensitivity of au-  
 364 totrophic versus heterotrophic processes will partially determine whether warming of the  
 365 near-surface ocean will bring about a net increase or decrease in the rate of export of  
 366 carbon to the deep ocean [Riebesell et al., 2009].

### 4.3. Modeling oceanic uptake

367 The findings herein support the hypothesis that the pattern of nitrate uptake in the  
 368 ocean is largely determined by the physiological trade-off between  $V_{\max}$  and  $A$  [Smith  
 369 et al., 2009], in combination with temperature. As in Smith [2010]: (1) the caveat applies  
 370 that biomass-specific rates may be less sensitive to temperature than the chlorophyll-  
 371 specific rates examined herein, but nevertheless (2) the difference between the inferred  
 372 temperature sensitivities with the Affinity model versus OU kinetics is an inescapable  
 373 result of the negative correlation between temperature and nutrient concentration in the  
 374 near-surface ocean, which will apply even for biomass-specific rates.

375 For large-scale modeling of the ocean, which generally does not resolve the short time  
 376 scales of the experiments analyzed herein, the assumption of instantaneous acclimation  
 377 is appropriate. Substituting Eq. (2) into the short-term approximations of Eqs. (4) and  
 378 (5), with  $S_a = S$ , gives the long-term (acclimated) response [Pahlow, 2005; Smith et al.,  
 379 2009] for uptake rate:

$$V_{OU} = \frac{V_0 S}{\left( \frac{V_0}{A_0} + 2\sqrt{\frac{V_0 S}{A_0}} + S \right)} \quad (11)$$

## 5. Conclusions

380 I find in this data set no evidence that the temperature sensitivities of affinity and  
381 maximum uptake rate differ, and therefore no evidence that half-saturation constants for  
382 nitrate uptake should depend on temperature. If this is the case in general, it would  
383 explain observations of a robust relationship between half-saturation constants, as fit to  
384 the MM equation, and the ambient nutrient concentration [Collos et al., 2005; Smith et al.,  
385 2009].

386 Although OU kinetics agrees better with the data set as a whole than does MM kinet-  
387 ics, there remains considerable room for improvement in the modeling of nitrate uptake  
388 kinetics, particularly with respect to the variability in  $V_{\max}$ . Further studies are warranted  
389 to seek better representations of the physiological trade-off(s) underlying the acclimation  
390 and adaptation of phytoplankton to nutrient concentrations.

391 Large-scale models of planktonic ecosystems and biogeochemical cycles should account  
392 explicitly for the combined effects of temperature and physiological acclimation (or evo-  
393 lutionary adaptation) to ambient nutrient concentrations. Smith et al. [2009], found that  
394 accounting for the physiological trade-off of OU kinetics in an Earth-system climate model  
395 made considerable differences in the projected response of marine productivity to global  
396 warming, even though they assumed the same temperature sensitivity for both MM and  
397 OU kinetics. Such large-scale modeling studies should also explore the use of greater  
398 temperature sensitivities for phytoplankton processes. Although the findings herein con-  
399 cern the overall ecological response, not the response for any particular species, they can  
400 inform the choice of trait-space and trade-offs in models that do resolve many different  
401 species or functional types [Follows and Dutkiewicz, 2011].

402 **Acknowledgments.** J. D. Annan and J. C. Hagreaves assisted with implementing the  
403 Adaptive Metropolis algorithm and interpretation of the results. Y. Yamanaka and A.  
404 Oshlies provided helpful suggestions. This work was supported by the Kakushin project  
405 of the Ministry of Education, Culture, Sports, Science and Technology (MEXT) of Japan.

## References

- 406 Akaike, H., 1974. A new look at the statistical model identification. IEEE Transactions  
407 on Automatic Control 19, doi:10.1109/TAC.1974.1100705, MR0423716.
- 408 Aksnes, D. L., Egge, J. K., 1991. A theoretical model for nutrient uptake in phytoplankton.  
409 Mar. Ecol. Prog. Ser. 70, 65–72.
- 410 Anderson, D. R., Burnham, K. P., Thompson, W. L., 2000. Null hypothesis testing:  
411 problems, prevalence, and an alternative. J. Wildlife Management 64, 912–923.
- 412 Armstrong, R. A., 1999. An optimization-based model of iron-light-ammonium colimita-  
413 tion of nitrate uptake. Limnol. Oceanogr. 44, 1436–1446.
- 414 Aumont, O., Maier-Reimer, E., Blain, S., Monfray, P., 2003. An ecosystem model of  
415 the global ocean including Fe, Si, P colimitations. Global Biogeochem. Cycles 17, doi:  
416 10.1029/2001GB001745.
- 417 Bissinger, J. E., Montagnes, D. J. S., Sharples, J., Atkinson, D., 2008. Predicting marine  
418 phytoplankton maximum growth rates from temperature: Improving on the eppley  
419 curve using quantile regression. Limnol. Oceanogr. 53 (2), 487–493.
- 420 Burnham, K. P., Anderson, D. R., 1998. Model Selection and Inference: A Practical  
421 Information-theoretic Approach. Springer-Verlag, New York.
- 422 Carlin, B. P., Louis, T. A., 1996. Bayes and Empirical Bayes Methods for Data Analysis,  
423 1st Edition. Monographs on Statistics and Applied Probability 69. Chapman & Hall,  
424 London.
- 425 Collos, Y., Vaquer, A., Souchu, P., 2005. Acclimation of nitrate uptake by phytoplankton  
426 to high substrate levels. J. Phycol. 41, 466–478.

- 427 Congdon, P., 2001. Bayesian Statistical Modeling. Wiley Series in Probability and Statis-  
428 tics. John Wiley & Sons, Ltd., Chichester.
- 429 Dauta, A., 1982. Conditions for phytoplankton development, comparative study of the  
430 behaviour of eight species in culture. ii. role of nutrients: assimilation and intracellular  
431 storage. *Annls. Limnol.* 18, 263–292.
- 432 Dugdale, R. C., 1967. Nutrient limitation in the sea: dynamics, identification, and signif-  
433 icance. *Limnol. Oceanogr.* 12, 685–695.
- 434 Eppley, R. W., 1972. Temperature and phytoplankton growth in the sea. *Fish. Bull.* 70,  
435 1063–1085.
- 436 Eppley, R. W., Rogers, J. N., McCarthy, J. J., 1969. Half-saturation constants for uptake  
437 of nitrate and ammonium by marine phytoplankton. *Limnol. Oceanogr.* 14, 912–920.
- 438 Fasham, M. J. R., Sarmiento, J. L., Slater, R. D., Ducklow, H. W., Williams, R., 1993.  
439 Ecosystem behaviour at bermuda station "S" and ocean weather station "india": A  
440 general circulation model and observational analysis. *Global Biogeochem. Cycles* 7,  
441 379–415.
- 442 Follows, M. J., Dutkiewicz, S., 2011. Modeling diverse communities of marine microbes.  
443 *Annu. Rev. Mar. Sci.* 3, 427–451.
- 444 Follows, M. J., Dutkiewicz, S., Grant, S., Chisholm, S. W., 2007. Emergent biogeography  
445 of microbial communities in a model ocean. *Science* 315, 1843–1846.
- 446 Gelman, A., Carlin, J. B., Stern, H. S., Rubin, D. B., 2004. Bayesian Data Analysis, 2nd  
447 Edition. Texts in Statistical Science. Chapman & Hall/CRC, Boca Raton.
- 448 Gentle, J. E., 2003. Random number generation and Monte Carlo methods, 2nd Edition.  
449 Statistics and Computing. Springer-Verlag, New York.

- 450 Goldman, J. C., Carpenter, E. J., 1974. A kinetic approach to the effect of temperature  
451 on algal growth. *Limnol. Oceanogr.* 19, 756–766.
- 452 Haario, H., Saksman, E., Tamminen, J., 2001. An adaptive Metropolis algorithm.  
453 *Bernoulli* 7, 223–242.
- 454 Harrison, P. J., Parslow, J. S., Conway, H. L., 1989. Determination of nutrient uptake  
455 kinetic parameters: a comparison of methods. *Mar. Ecol. Prog. Ser.* 52, 301–312.
- 456 Harrison, W. G., Harris, L. R., Irwin, D. B., 1996. The kinetics of nitrogen utilization in  
457 the oceanic mixed layer: Nitrate and ammonium interactions at nanomolar concentra-  
458 tions. *Limnol. Oceanogr.* 41, 16–32.
- 459 Healey, F. P., 1980. Slope of the Monod equation as an indicator of advantage in nutrient  
460 competition. *Microbial Ecology* 5, 281–286.
- 461 Healy, M., 1968a. Inversion of a positive semi-definite matrix. *Appl. Stat.* 17, 198–199.
- 462 Healy, M., 1968b. Triangular decomposition of a symmetric matrix. *Appl. Stat.* 17, 195–  
463 197.
- 464 Kanda, J., Saino, T., Hattori, A., 1985. Nitrogen uptake by natural populations of phy-  
465 toplankton and primary production in the Pacific ocean: regional variability of uptake  
466 capacity. *Limnol. Oceanogr.* 30, 987–999.
- 467 Kishi, M. J., Eslinger, D. L., Kashiwai, M., Megrey, B. A., Ware, D. M., Werner, F. E.,  
468 Aita-Noguchi, M., Azumaya, T., Fujii, M., Hashimoto, S., Iizumi, H., Ishida, Y., Kang,  
469 S., Kantakov, G. A., Kim, H., Komatsu, K., Navrotsky, V. V., Smith, S. L., Tadokoro,  
470 K., Tsuda, A., Yamamura, O., Yamanaka, Y., Yokouchi, K., Yoshie, N., Zhang, J.,  
471 Zuenko, Y. I., Zvalinsky, V. I., 2007. NEMURO: Introduction to a lower trophic level  
472 model for the North Pacific marine ecosystem. *Ecol. Model.* 202, 12–25.

- 473 Laine, M., 2008. Adaptive MCMC methods with applications in environmental and geo-  
474 physical models. Ph.D. thesis, Lappeenranta University of Technology, Lappeenranta,  
475 Finland.
- 476 LeQuere, C., Harrison, S. P., Prentice, I. C., Buitenhuis, E. T., Aumont, O., Bopp, L.,  
477 Claustre, H., da Cunha, L. C., Geider, R., Giraud, X., Klaas, C., Kohfeld, K. E., Leg-  
478 endre, L., Manizza, M., Platt, T., Rivkin, R. B., Sathyendranath, S., Uitz, J., Watson,  
479 A. J., Wolf-Gladrow, D., 2005. Ecosystem dynamics based on plankton functional types  
480 for global ocean biogeochemistry models. *Global Change Biology* 11, 2016–2040.
- 481 Marinov, I., Follows, M., Gnanadesikan, A., Sarmiento, J. L., Slater, R. D., 2008. How  
482 does ocean biology affect atmospheric pco<sub>2</sub>? Theory and models. *J. Geophys. Res.* 113,  
483 doi: 10.1029/2007JC004598.
- 484 Moisan, J. R., Moisan, T. A., Abbott, M. R., 2002. Modelling the effect of temperature on  
485 the maximum growth rates of phytoplankton populations. *Ecol. Model.* 153, 197–215.
- 486 Pahlow, M., 2005. Linking chlorophyll-nutrient dynamic to the Redfield N:C ratio with a  
487 model of optimal phytoplankton growth. *Mar. Ecol. Prog. Ser.* 287, 33–43.
- 488 Parekh, P., Follows, M. J., Boyle, E. A., 2005. Decoupling of iron and phosphate in the  
489 global ocean. *Global Biogeochem. Cycles* 19, doi: 10.1029/2004GB002280.
- 490 Pomeroy, L. R., Wiebe, W. J., 2001. Temperature and substrates as interactive limiting  
491 factors for marine heterotrophic bacteria. *Aquat. Microb. Ecol.* 23, 187–204.
- 492 Riebesell, U., Körtzinger, A., Oschlies, A., 2009. Sensitivities of marine carbon fluxes to  
493 ocean change. *Proc. Natl. Acad. Sci.* 109, doi: 10.1073/pnas.0813291106, 20602–20609.
- 494 Schwarz, G. E., 1978. Estimating the dimension of a model. *Ann. Statist.* 6, 461–464.

- 495 Silio-Calzada, A., Bricaud, A., Gentili, B., 2008. Estimates of sea surface nitrate concen-  
496 trations from sea surface temperature and chlorophyll concentration in upwelling areas:  
497 A case study for the Benguela system. *Remote Sens. Environ.* 112, 3173–3180.
- 498 Smith, S. L., 2010. Untangling the uncertainties about combined effects of temperature  
499 and concentration on nutrient uptake rates in the ocean. *Geophys. Res. Lett.* 37, L11603,  
500 doi:10.1029/2010GL043617.
- 501 Smith, S. L., Yamanaka, Y., Pahlow, M., Oschlies, A., 2009. Optimal Uptake kinetics:  
502 physiological acclimation explains the pattern of nitrate uptake by phytoplankton in  
503 the ocean. *Mar. Ecol. Prog. Ser.* 384, 1–12, doi: 10.3354/meps08022.
- 504 Yamanaka, Y., Tajika, E., 1996. The role of the vertical fluxes of particulate organic  
505 matter and calcite in the oceanic carbon cycle: Studies using an ocean biogeochemical  
506 general circulation model. *Global Biogeochem. Cycles* 10, 361–382.

507 **Figure Captions**

508 **Fig. 1: Relationship between observed ambient temperature ( $T$ ) and nitrate**  
 509 **concentration ( $[\text{NO}_3]$ )** for the data set of Harrison et al. [1996]. The line is the linear  
 510 log-log regression:  $\log[\text{NO}_3] = 277 - 92.8 \log T$  ( $r^2 = 0.60$ ,  $F = 85.5$ ,  $n = 60$ ,  $p < 10^{-12}$ ).

511 **Fig. 2: Kinetic parameters for nitrate uptake versus temperature, assum-**  
 512 **ing separate values of temperature sensitivities.** Modeled and observed values of  
 513 maximum uptake rate ( $V_{\text{max}}$ ), affinity ( $A$ ), and corresponding half-saturation “constants”  
 514 ( $K_s$ ). Modeled values of  $K_s$  were calculated as  $V_{\text{max}}/A$ . The two models, respectively,  
 515 assume either (left column: A, C, E) no physiological trade-off (Affinity model), or (right  
 516 column: B, D, F) the physiological trade-off specified by the OU model. For each best-fit  
 517 model value (red diamonds), vertical lines show the 95 % quantile range from the ensemble  
 518 of parameter values (solid lines), and the 95 % quantile range of predicted observations,  
 519 based on the ensemble of standard errors (dotted lines). Solid blue lines show the effect  
 520 of temperature alone, using the best-fit parameters for each model, respectively. With  
 521 the Affinity model, modeled values depend only on temperature, but with the OU model  
 522 they also depend on ambient nutrient concentration (not shown).

523 **Fig. 3: Kinetic parameters for nitrate uptake versus temperature, assuming**  
 524 **the same temperature sensitivity for maximum uptake rate and affinity.** As in  
 525 Fig. 1, but fits of models were conducted assuming the same temperature sensitivity for  
 526  $V_{\text{max}}$  and  $A$  within each model, respectively.

527 **Fig. 4: Kinetic parameters for nitrate uptake versus ambient nitrate concen-**  
 528 **tration, assuming the same temperature sensitivity for maximum uptake rate**  
 529 **and affinity.** As in Fig. 2, except plotted versus ambient nitrate concentration.

**Figure Captions** (continued)

Fig. 5: **Estimated *in situ* nitrate uptake rates based on observed ambient nitrate concentrations.** Calculated using either reported values of uptake parameters from the ship-board incubations using graded nutrient additions of Harrison et al. [1996] (black circles) or the best-fits of models for variation in those parameters (red diamonds) assuming either (A) no physiological trade-off (Affinity model) or (B) the physiological trade-off specified by OU kinetics. Vertical lines show 95 % quantile ranges of modeled rates calculated from the ensemble of parameter values. Correlations between the estimated rates from the models and those estimated from the reported kinetic parameters are indistinguishable at  $r^2 = 0.51$  ( $F = 48.1$  for the Affinity model vs.  $F = 48.5$  for the OU model;  $n = 48$  and  $p < 10^{-7}$  for both).

**Table 1. Results of AM fits of equations to the data.** For kinetic parameters and estimated standard errors ( $\sigma$ , from Gibbs sampling), the mean (standard deviation in parentheses) is reported over the ensemble of  $64 \times 10^6$  simulations for each model, respectively. Values of rate coefficients are for a reference temperature of 293 K. LL is the ensemble mean log likelihood. Akaike Information Criteria (AIC) Akaike [1974] are calculated from Eq. (8) based on this LL, the number of parameters fitted, and the number of observations.

---

Assuming distinct temperature sensitivities for $V_{\max}$ and $A$		
	Affinity model	OU model
Parameter (units)		
$V_{\max, r}$ (nmol h <sup>-1</sup> ( $\mu$ g Chl) <sup>-1</sup> )	10.3 (1.12)	-
$V_{0, r}$ (nmol h <sup>-1</sup> ( $\mu$ g Chl) <sup>-1</sup> )	-	32.7 (7.31)
$A_r$ (L h <sup>-1</sup> ( $\mu$ g Chl) <sup>-1</sup> )	0.386 (0.073)	-
$A_{0, r}$ (L h <sup>-1</sup> ( $\mu$ g Chl) <sup>-1</sup> )	-	0.792 (0.180)
$E_{a,V}/R$ (K)	4,470 (1,080)	10,000 (1,580)
$E_{a,A}/R$ (K)	15,300 (3,240)	6,750 (3,500)
Other posterior quantities		
$\sigma_{\log_{10} V_{\max}}$	0.333 (0.032)	0.362 (0.034)
$\sigma_{\log_{10} A}$	0.560 (0.058)	0.514 (0.056)
LL	-73.8	-74.4
AIC	156	157

Assuming the same temperature sensitivity for $V_{\max}$ and $A$		
	Affinity model	OU model
Parameter (units)		
$V_{\max, r}$ (nmol h <sup>-1</sup> ( $\mu$ g Chl) <sup>-1</sup> )	10.8 (1.14)	-
$V_{0, r}$ (nmol h <sup>-1</sup> ( $\mu$ g Chl) <sup>-1</sup> )	-	31.2 (6.65)
$A_r$ (L h <sup>-1</sup> ( $\mu$ g Chl) <sup>-1</sup> )	0.378 (0.077)	-
$A_{0, r}$ (L h <sup>-1</sup> ( $\mu$ g Chl) <sup>-1</sup> )	-	0.795 (0.20)
$E_a/R$ (K)	5,440 (1,060)	9,380 (1,250)
Other posterior quantities		
$\sigma_{\log_{10} V_{\max}}$	0.336 (0.031)	0.367 (0.035)
$\sigma_{\log_{10} A}$	0.610 (0.064)	0.508 (0.054)
LL	-72.5	-68.7
AIC	151	144

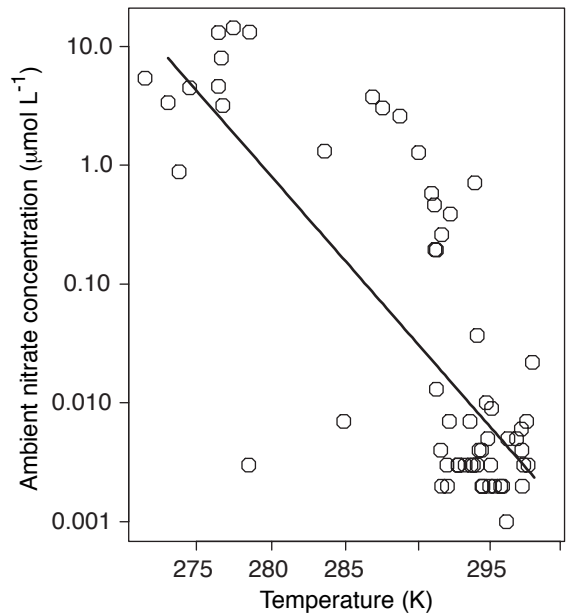
---

**Table 2.** Number of parameters fitted ( $p$ ), Akaike Information Criteria (AIC), difference in AIC ( $\Delta_{AIC}$ ), and the resulting Akaike weights ( $w$ ) from Eq. (10), which are the relative normalized (0, 1) probabilities for each of the four models considered.

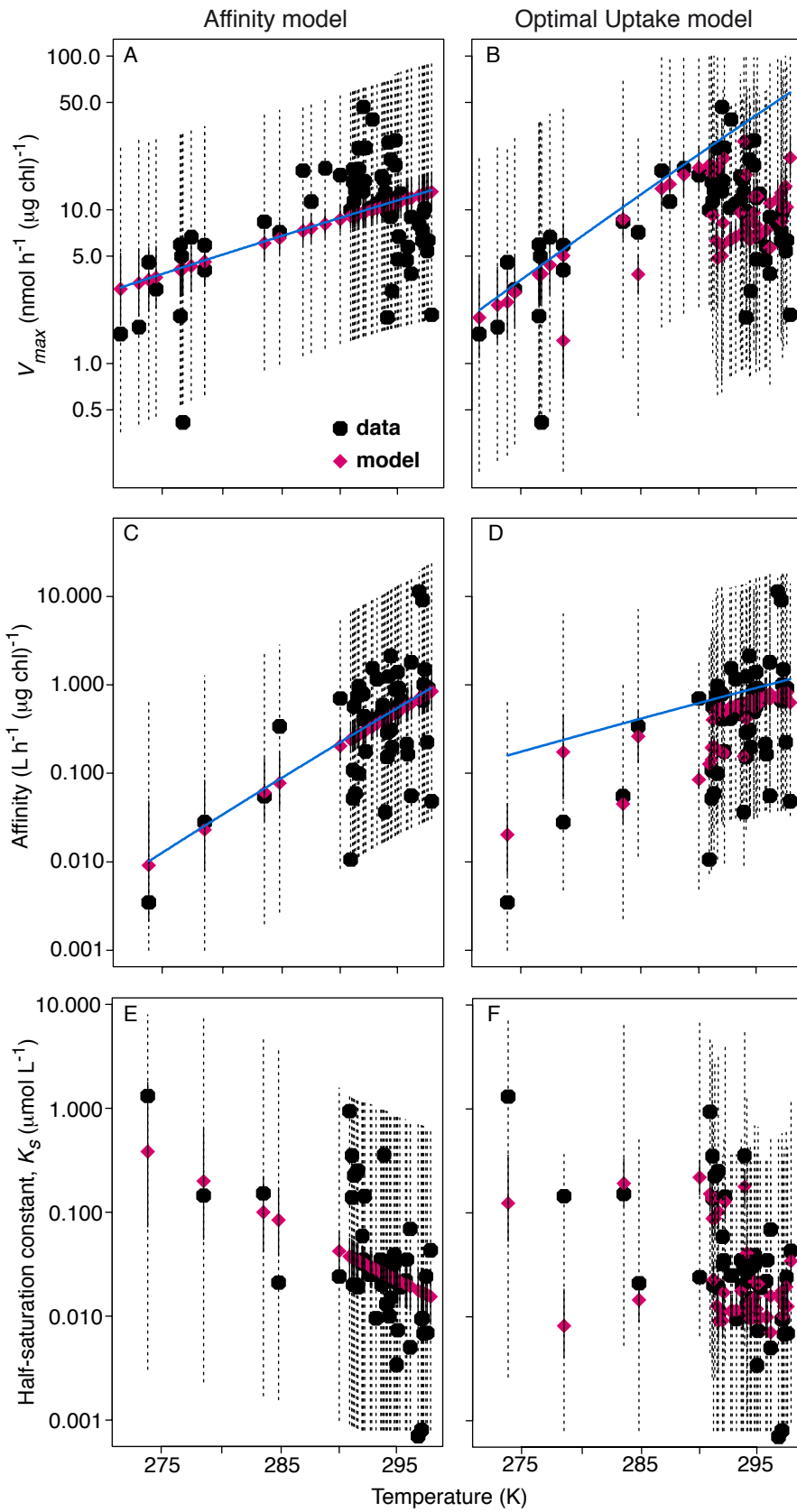
model	$p$	AIC	$\Delta_{AIC}$	$w$
Affinity model, distinct $T$ sensitivities	4	156.0	12.42	0.0020
Affinity model, identical $T$ sensitivities	3	151.2	7.620	0.0216
OU model, distinct $T$ sensitivities	4	157.2	13.64	0.0010
OU model, identical $T$ sensitivities	3	143.6	0	0.9753

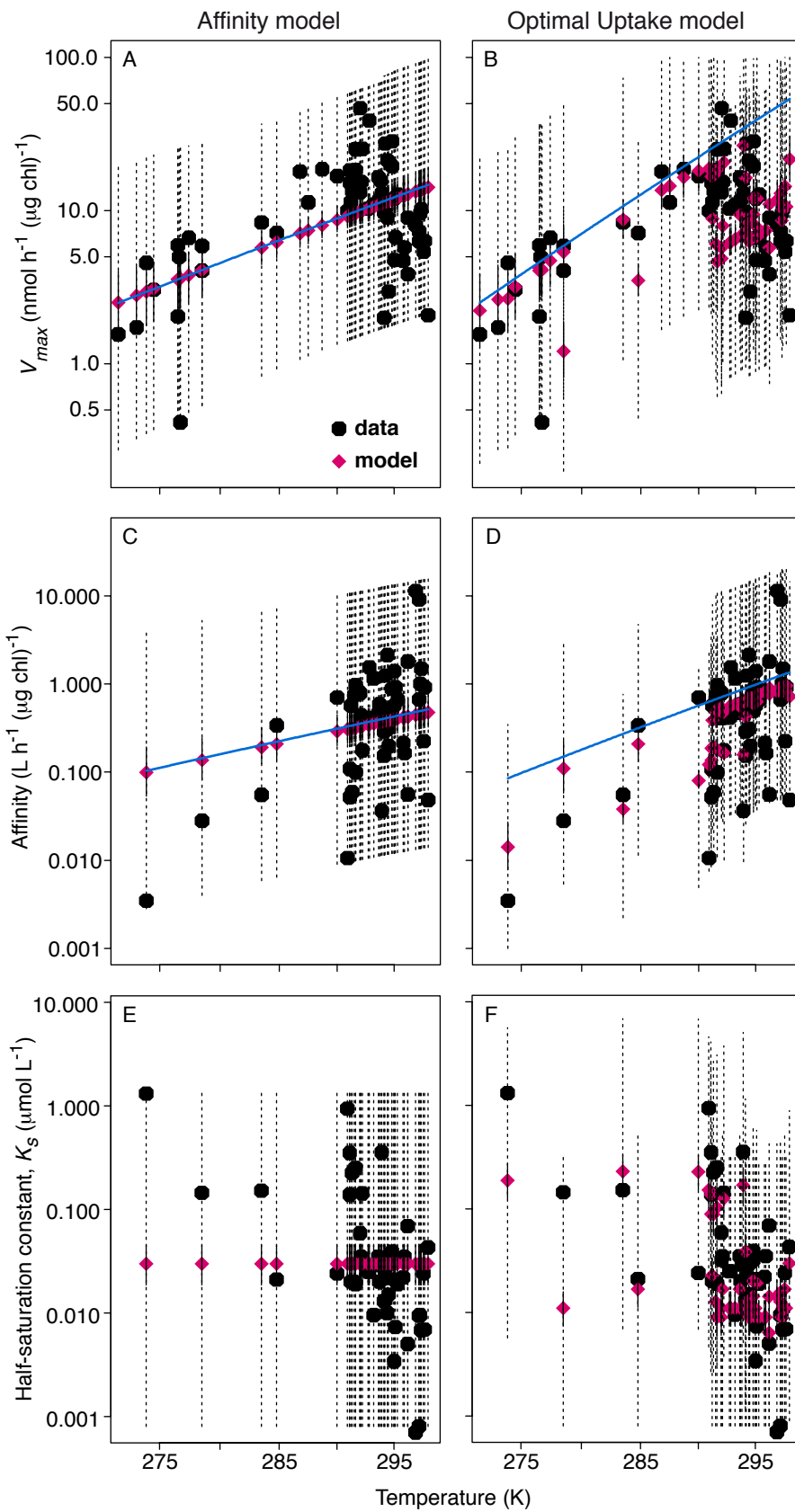
**Table 3.** Correlation coefficients,  $r^2$  (p-values in parentheses) of best-fit model output with the corresponding observations.

Assuming distinct temperature sensitivities for $V_{\max}$ and $A$		
Observable (no. of observations)	Affinity model	OU model
$V_{\max}$ ( $N = 60$ )	0.22 ( $2 \times 10^{-4}$ )	0.18 ( $6 \times 10^{-4}$ )
$A$ ( $N = 48$ )	0.33 ( $2 \times 10^{-5}$ )	0.47 ( $8 \times 10^{-8}$ )
$K_s$ ( $N = 48$ )	0.35 ( $1 \times 10^{-5}$ )	0.39 ( $2 \times 10^{-6}$ )
Assuming the same temperature sensitivity for $V_{\max}$ and $A$		
Observable (no. of observations)	Affinity model	OU model
$V_{\max}$ ( $N = 60$ )	0.22 ( $2 \times 10^{-4}$ )	0.16 ( $2 \times 10^{-3}$ )
$A$ ( $N = 48$ )	0.33 ( $2 \times 10^{-5}$ )	0.47 ( $7 \times 10^{-8}$ )
$K_s$ ( $N = 48$ )	0.00 ( 1 )	0.43 ( $4 \times 10^{-7}$ )

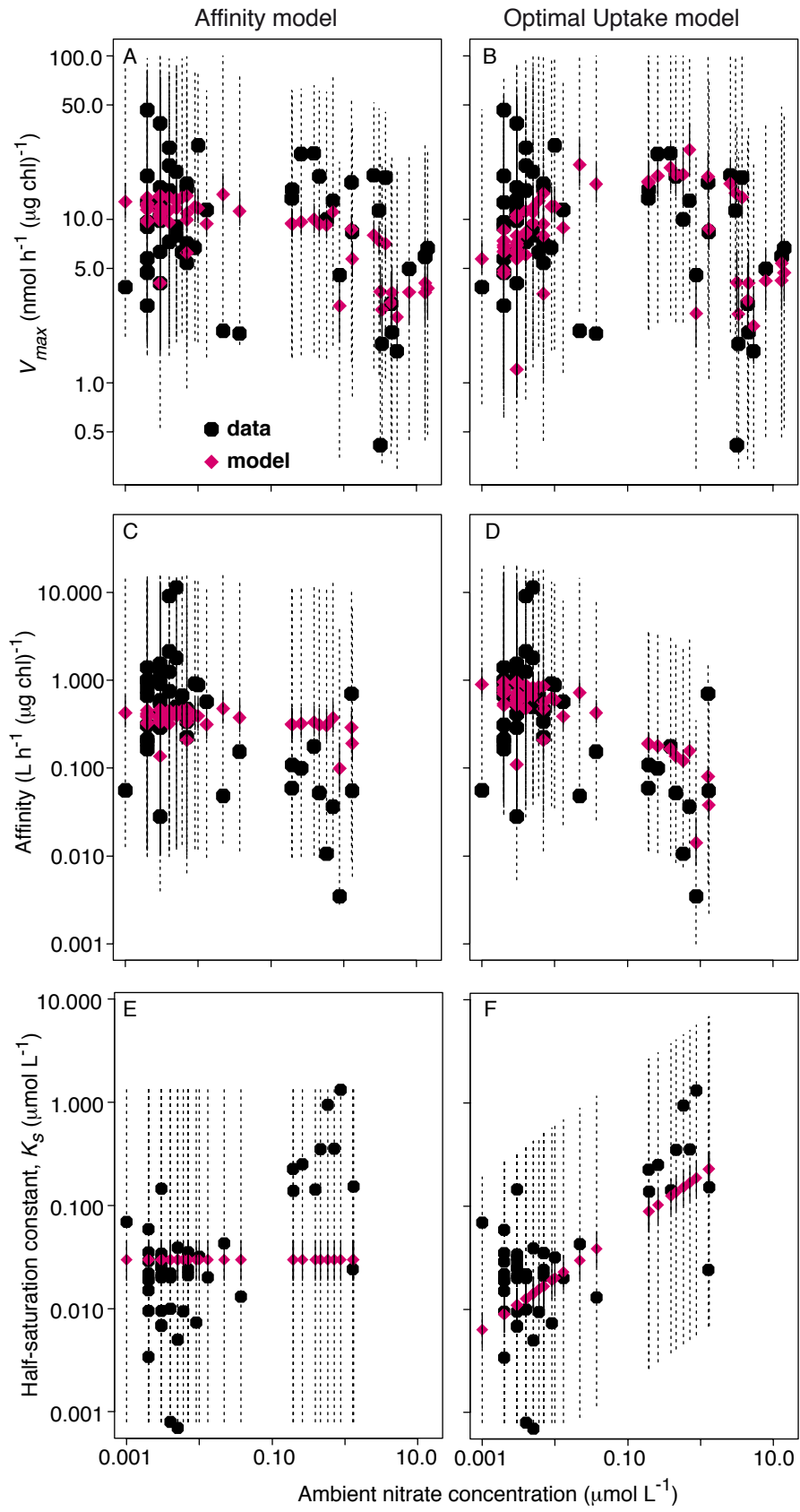


Smith. Fig. 1





Smith. Fig. 3



Smith. Fig. 4

